to ensure convergence of small exchange factors (which applies for the high-emissivity enclosures studied here).

Specular and Bi-directional Reflections. These were examined for $\epsilon_e = 0.1$ and $\epsilon_e = 0.5$, with $\epsilon_o = 0.9$. A one-bounce approximation was used to calculate the transition probabilities. An analytic bi-directional reflection function presented by Billings et al. (1991) was employed:

$$f(\theta_I, \theta_R) = \frac{(s^2 + 1)\cos(\theta_R)e^{-s|\theta_I+\theta_R|}}{2s\cos(\theta_I) + e^{-s(\pi/2+\theta_I)} + e^{-s(\pi/2-\theta_I)}}$$

$$-\pi/2 \geq \theta \geq \pi/2. \quad (5)$$

The parameter s controls the specularity of the reflected radiation. Setting $s = 0$ results in diffuse reflection, but as $s \to \infty$ reflection becomes increasingly specular. Simulations were performed with $s = 4$, which yields a "directional-diffuse" reflection characteristic.

To calculate exchange factors (in MC) and transition probabilities (in DFMC) directions need to be sampled from the CDF of Eq. (5). The CDF must be inverted and stored as a lookup table of reflected directions corresponding to possible incident directions and random number values (Maltby and Burns, 1991; Modest, 1993). Cubic spline interpolation (Press et al., 1992) was employed to tabulate reflected directions in degree intervals of incident direction and percent intervals in random number values. Actual angles of reflection were obtained by linear interpolation from the lookup table.

For specular reflection DFMC was approximately eight times faster than MC, while for bi-directional reflection this increase was sixfold when $\epsilon_e = 0.1$ and about threefold when $\epsilon_e = 0.5$. Again, there is strong agreement between the two approaches (Figs. 3 and 4). For specular reflection, there is a slight difference in the exchange factors calculated by each method to faces "a" and "c" (Fig. 3). The accuracy of these results could be improved by increasing the number of bounces of radiation when calculating the transition probabilities or by optimising the surface sizes.

Conclusion

A numerical approach has been presented that offers faster calculation of exchange factors in nonblack enclosures. For the studied cases, predictions from the DFMC and MC methods are in close agreement, and computational speeds were improved by factors of between 2.6 and 10.4 by using the DFMC method. The DFMC model is easy to implement, and transition probabilities can be determined by existing computer codes. Furthermore, because the transition probabilities represent directional exchange between surfaces they can be reused. This provides a significant advantage if the surface absorptivities, or the directional properties of only a few surfaces, are altered for the purpose of analysis.

Work is continuing with the development of the method in three areas. First, to provide a broader understanding of its performance characteristics (particularly when applied to realistic three-dimensional geometries). Secondly, to investigate means for optimizing the calculation of specular and bi-directional reflections. And thirdly, because the present approach is memory intensive (particularly for calculations including bi-directional reflections), to develop improved algorithms for managing the CDF matrices (e.g., sparse matrix routines, data compression, and function approximation).

References

Bevans, J. T., and Edwards, D. K., 1965, "Radiation Exchange in an Enclosure with Directional Wall Properties," ASME JOURNAL OF HEAT TRANSFER, Vol. 87, pp. 388–396.

Billings, R. L., Barnes, J. W., and Howell, J. R., 1991, "Markov Analysis of Radiative Transfer in Enclosures With Bidirectional Reflections," *Numerical Heat Transfer*, Part A, Vol. 19, pp. 313–326.

Maltby, J. D., and Burns, P. J., 1991, "Performance, Accuracy, and Convergence in a Three-Dimensional Monte Carlo Radiative Heat Transfer Simulation," *Numerical Heat Transfer*, Part B, Vol. 19, pp. 191–209.

Modest, M. F., 1993, *Radiative Heat Transfer*, McGraw-Hill, New York.

Press, W. H., Flannery, B. P., Teukolsky, S. A., and Vetterling, W. T., 1992, *Numerical Recipes*, 2nd. Ed., Cambridge University Press, Cambridge, England.

Shaughnessy, B. M., 1996, "Radiative Heat Transfers in Low-Emissivity Enclosures," Ph.D. thesis, School of Mechanical Engineering, Cranfield University, England.

Siegel, R., and Howell, J. R., 1972, *Thermal Radiation Heat Transfer*, McGraw-Hill, New York.

Weiner, M. M., Tindall, J. W., and Candell, L. M., 1965, "Radiative Interchange Factors by Monte-Carlo," ASME Paper No. 65-WA/HT-51.

Heat Transfer Coefficient Enhancement With Perforated Baffles

S. Dutta,[1,2] P. Dutta,[1] R. E. Jones,[1] and J. A. Khan[1,2]

Introduction

Primarily there are three popular techniques to enhance heat transfer coefficient in channels: (i) boundary layer disturbance that is created by periodically placed ribs on the heat transfer surface; (ii) impingement cooling that uses high velocity jets to cool the surface of interest; and (iii) internal flow swirls or tape twisters that create a significant amount of bulk flow disturbance. Inclined solid baffles may be considered as a combination of ribs and channel inserts. Baffles are big enough to disturb the core flow, but like ribs, they are mounted on or near the heat transfer surface and can be spatially periodic. Perforations in inclined baffles create multiple jet impingement condition, and thus create a situation where all three major heat transfer coefficient enhancement techniques work in unison. In the past, experimental results were published with baffle plates perpendicular to the flow direction. Habib et al. (1994) have investigated heat transfer and flow over perpendicular baffles of various heights. Unlike previous publications, in our present study, we investigate heat transfer enhancement using an *inclined* baffle. The baffle plate is oriented in both stream aligned and stream opposed directions. In addition, jet impingement is added by using multiple jet hole arrays. Since the baffle is inclined, the jets can be directed toward the heat transfer surface. Characteristic friction factors and average Nusselt numbers with these inclined baffles are discussed in Dutta et al. (1997).

Experimental Facility

A suction mode blower is used to draw air through a rectangular cross-sectioned wind tunnel. The cross section of the smooth wind tunnel is 24.92 cm × 4.92 cm (channel height, H = 4.92 cm). Air enters the tunnel through a contraction and flow straighteners, and then the flow develops through a 31 H-long unheated entrance. The exit is at a 22.2 H distance downstream of the heated test section. The heated test section is 19.2 H

[1] Department of Mechanical Engineering, University of South Carolina, Columbia, SC 29208.

[2] Mem. ASME.

Contributed by the Heat Transfer Division for publication in the JOURNAL OF HEAT TRANSFER and presented at '97 IMECE, Dallas. Manuscript received by the Heat Transfer Division, Aug. 1, 1997; revision received, Mar. 20, 1998. Keywords: Enclosure Flows, Flow Separation, Forced Convection, Heat Exchangers, Turbulence. Associate Technical Editor: J. C. Han.

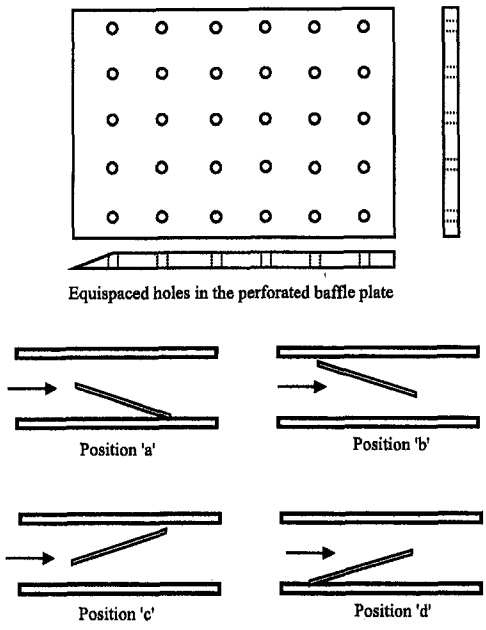

Fig. 1 Perforated baffle plate and four different inclined baffle positions

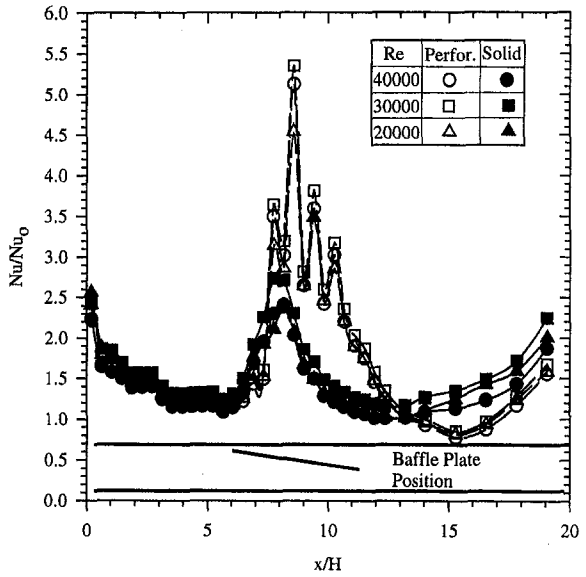

Fig. 3 Local Nusselt number ratio distribution along the channel centerline for perforated and solid baffles at position "*b*"

long, and the top surface is heated and instrumented. Other three sides are unheated and insulated. Stainless steel foil heaters are aligned perpendicular to the flow direction, similar to the configuration used by Han (1988). The thermocouples are laid along the centerline of the channel, and each strip is equipped with one thermocouple. Seven-mm diameter turbulators are located at 1.55 H upstream and 2.3 H downstream of the test section.

The solid and perforated baffle plates used are 28.9 cm long, 5 mm thick, and span the entire channel (24.92 cm). Leading edges of the baffle plates are kept sharp to reduce the flow disturbance by the protruding edge. Perforations hole diameters are D = 1.07 cm and center to center hole spacing is 3.56 D. Four different baffle plate positions with respect to the top heated surface are used. The baffle plate and its various positions are shown in Fig. 1. The heating starts at $6H$ upstream of the leading edge of the inclined baffle. The angle of inclination is 5 deg. When the baffle is mounted near the top heated surface, a gap of 3 mm between the heater surface and the baffle is maintained to avoid flow stagnation where the baffle plate contacts the channel wall. The solid baffle creates a blockage ratio of 65 percent and perforated baffles create a lower blockage due to the holes in the baffle.

The local centerline heat transfer coefficient, h, is calculated from heat flux, and wall and bulk fluid temperatures. The heat flux, q'', is the supplied electrical power divided by the total heater surface area. The heat loss is estimated from a separate heat loss experiment done on the test facility without airflow. A characteristic heat loss curve is developed for each thermocouple location. It is found that the maximum local heat flux loss, q''_{loss}, is less than six percent of the total supplied local heat flux, q''. The centerline wall temperatures are measured directly by thermocouples; and the bulk temperature is calculated by control volume energy balance technique (heat carried by the air stream). The channel centerline Nusselt number is

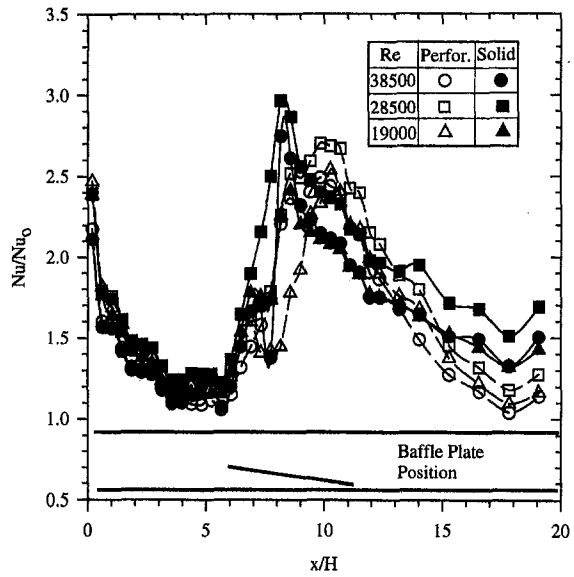

Fig. 2 Local Nusselt number ratio distribution along the channel centerline for perforated and solid baffles at position "*a*"

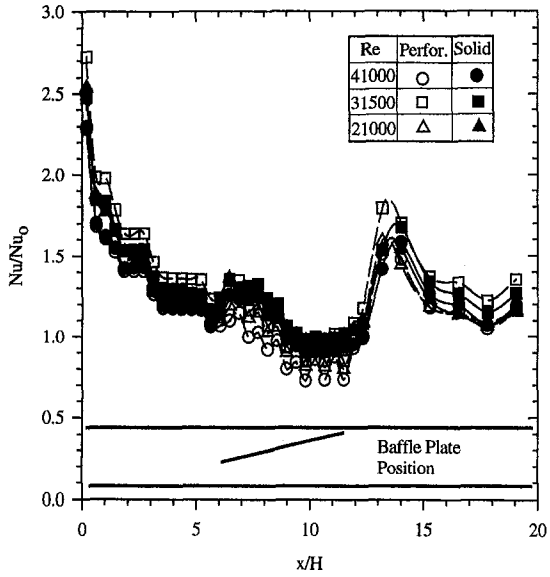

Fig. 4 Local Nuselt number ratio distribution along the channel centerline for perforated and solid baffles at position "*c*"

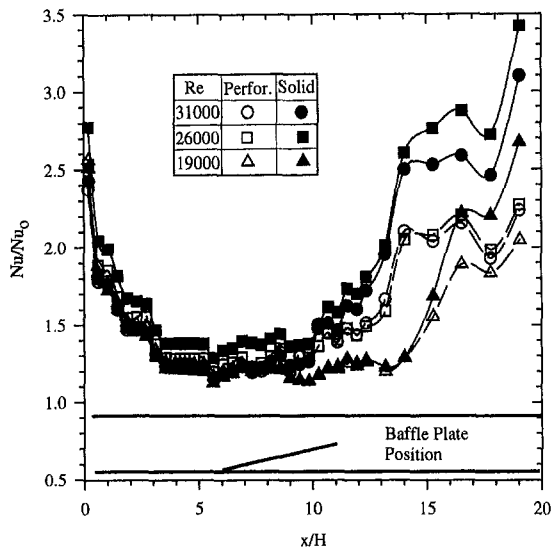

Fig. 5 Local Nusselt number ratio distribution along the channel centerline for perforated and solid baffles at position "*d*"

calculated from the heat transfer coefficient and the channel height as: $Nu = hH/K_{air}$. The Nusselt numbers are normalized to minimize the Reynolds number effect by Nu_o, Nusselt number for fully developed pipe flow at the same Reynolds number, Re. The Nu_o is a function of Re and Prandtl number, Pr, and given by Dittus-Boelter Equation as $Nu_o = 0.023\ Re^{0.8}\ Pr^{0.4}$ (Incropera and DeWitt, 1990). Maximum uncertainty estimate on the flow Reynolds number, based on channel centerline velocity and channel height, is ±2 percent and maximum uncertainty in Nusselt number, Nu, is ±3 percent.

Results and Discussion

Figures 2 to 5 show the Nusselt number ratios, Nu/Nu_o, for different baffle plate orientations. Four different positions of the baffle plate are considered, as shown in the figures (also see Fig. 1). Both solid and perforated plate results are plotted in the same graph. The Nusselt number ratio presented signifies the amount of improvement in the heat transfer coefficient obtained by the flow disturbance promoters. While verifying the test facility and instrumentation, a smooth channel Nusselt number ratio profile showed that the developed channel centerline Nusselt number ratio was within 1.1 and 1.2 at locations downstream of $x/H = 5$ at Re = 30,000. Figure 2 shows the Nusselt number distribution along the centerline of the channel for orientation "*a*." Initially high values of the Nusselt number ratio are due to the start of the thermal boundary layer. The Nusselt number ratio gradually decreases to nearly fully developed value before being affected by the baffle plate. The heat transfer coefficient enhancement starts immediately upstream of the baffle plate location. Results with the solid plate are higher than the perforated plate for the given configuration. The solid plate creates a flow blockage and increases the local flow velocity at the start of the baffle plate. The Nusselt number ratio peaks downstream of the maximum flow blockage. It can be argued that the flow separates in the diverging channel, and therefore, the heat transfer coefficient increases. The diverging portion of the channel indicates an increased heat transfer coefficient. The perforated plate allows some fluid to pass through the plate and increases mixing in the core flow. The maximum Nusselt number location shifts downstream with the addition of perforation and the magnitude of the Nusselt number ratio is also low in most locations with the perforated baffle plate compared to that with the solid baffle.

Figure 3 shows results for configuration "*b*" of the baffle plate. Unlike other three configurations, perforations improve the heat transfer coefficient in this baffle orientation. In the perforated plate, flow through holes act as impingement jets and heat transfer coefficient is significantly improved. Interestingly, the heat transfer downstream of the baffle plate is higher for the solid plate. The higher heat transfer coefficients at the end of the test section may be due to flow reattachment downstream of the baffle plate.

Figure 4 shows that the blockage created by the baffle in orientation "*c*" is not favorable for heat transfer enhancement. The flow leaks through the gap between the baffle plate and the heat transfer surface and there is a local peak near the end of the baffle plate. Perforated plate performs worse than the solid plate at the plate bounded region. Figure 5 shows configuration "*d*" of the baffle plate. The flow accelerates due to the channel constriction created by the inclined baffle. However, the Nusselt number ratio is higher in all downstream locations of the inclined baffle. Heat transfer coefficient enhancement at the downstream locations may be coupled to the wake shed by the baffle. The perforated plate performs poorly compared to the solid plate in heat transfer augmentation. Since the perforated holes allow the flow to leak through the blockage, wakes shed by perforated baffle plate are weaker than wakes generated by the solid baffle.

References

Dutta, S., Dutta, P., Jones, R. E., and Khan, J. A., 1997, "Experimental Study of Heat Transfer Coefficient Enhancement with Inclined Solid and Perforated Baffles," ASME IMECE, Dallas, TX, Nov. 16–21, ASME Paper No. 97-WA/HT-4.

Habib, M. A., Mobarak, A. M., Sallak, M. A., Abdel Hadi, E. A., and Affify, R. I., 1994, "Experimental Investigation of Heat Transfer and Flow Over Baffles of Different Heights," ASME JOURNAL OF HEAT TRANSFER, Vol. 116, pp. 363–368.

Han, J. C., 1988, "Heat Transfer and Friction Characteristics in Rectangular Channels With Rib Turbulators," ASME JOURNAL OF HEAT TRANSFER, Vol. 110, pp. 321–328.

Incropera, F. P., and DeWitt, D. P., 1990, *Fundamentals of Heat and Mass Transfer*, 3rd Ed., John Wiley and Sons, New York, p. 496.

Second-Law Analysis on Wavy Plate Fin-and-Tube Heat Exchangers

W. W. Lin[1] and D. J. Lee[1,2]

Second-law analysis on the herringbone wavy plate fin-and-tube heat exchanger was conducted on the basis of correlations of Nusselt number and friction factor proposed by Kim et al. (1997), from which the entropy generation rate was evaluated. Optimum Reynolds number and minimum entropy generation rate were found over different operating conditions. At a fixed heat duty, the in-line layout with a large tube spacing along streamwise direction was recommended. Furthermore, within the valid range of Kim et al.'s correlation, effects of the fin spacing and the tube spacing along spanwise direction on the second-law performance are insignificant.

[1] Department of Chemical Engineering, National Taiwan University, Taipei, Taiwan 10617, R. O. China.

[2] Corresponding author. e-mail: djlee@ccms.ntu.edu.tw.

Contributed by the Heat Transfer Division for publication in the JOURNAL OF HEAT TRANSFER. Manuscript received by the Heat Transfer Division, Dec. 15, 1997; revision received, May 4, 1998. Keywords: Finned Surfaces, Heat Transfer, Optimization, Thermodynamics. Associate Technical Editor: B. T. F. Chung.